NMR Spectroscopy

DOI: 10.1002/anie.201100310

Structure, Dynamics, and Kinetics of Weak Protein–Protein Complexes from NMR Spin Relaxation Measurements of Titrated Solutions**

Loïc Salmon, José-Luis Ortega Roldan, Ewen Lescop, Antoine Licinio, Nico van Nuland, Malene Ringkjøbing Jensen, and Martin Blackledge**

Almost all cellular mechanisms are controlled by protein–protein interactions, and the dynamic and kinetic properties of these interactions determine cellular function.[1,2] Weak or transient protein–protein interactions, with equilibrium dissociation constants approaching millimolar ranges, are known to control numerous biological processes, including transcription, replication, and signal transduction. NMR spectroscopy is an essential tool for the study of molecular complexes because of its extraordinary sensitivity to interactions whose affinities may vary over many orders of magnitude. Although NMR spectroscopy can in theory be used to study ultraweak complexes, they remain the least well-characterized complexes in terms of molecular structure and dynamics.[3,4]

The key problem with studying low-affinity complexes is that the weakness of the interaction precludes the measurement of parameters that originate uniquely from the bound form of either protein when working with experimentally accessible concentrations. Although chemical shift titration provides information identifying the molecular interface,[5] more precise structural information that determines the relative orientation of the two partners is difficult to measure in such systems. The study of local flexibility in the bound forms of weak complexes is also essential for the understanding of the role and the specificity of the intrinsic motions in molecular recognition[6–8] but again requires the measurement of data that unambiguously derive from the complexed forms of the protein.

We have recently presented a titration approach for the determination of residual dipolar couplings (RDCs) from experimentally inaccessible complexes.[9] Here, we extend this approach to the measurement of ^{15}N spin relaxation rates and demonstrate that this can provide long-range structural, dynamic, and kinetic information about these elusive systems.

Spin relaxation is a particularly attractive tool for the study of protein complexes because it characterizes both internal dynamics and long-range order from R_2/R_1 ratios ($R_1 =$ longitudinal relaxation rate, $R_2 =$ transverse relaxation rate).[10–15] Here, we combine titration and ^{15}N relaxation measurements to study the weakly interacting complex between ubiquitin (Ub) and the third SH3 domain from the human CD2 adapter protein (SH3).[16] We estimate the dissociation constant (K_D) for this interaction to be (190 ± 74) μM at 35 °C, such that measurement of NMR parameters under saturating conditions of either of the partners is not readily feasible. This is a particular problem for the interpretation of spin relaxation where mixtures of free and bound forms of the proteins may contribute very differently to the measured relaxation rates, both in terms of the dipolar and the chemical shift anisotropy (CSA) relaxation mechanisms, and because of chemical shift exchange in the interaction site. To accurately isolate these contributions, longitudinal and transverse ^{15}N relaxation rates were measured for different mixtures of the two partners. The ^{15}N heteronuclear single quantum coherence (HSQC) spectra collected from mixtures of the two ^{15}N-labeled proteins were highly dispersed, such that ^{15}N relaxation rates could be measured simultaneously for both proteins in a single sample. Data measured at 600 MHz are shown in Figure 1 for three mixtures (p1, p2, and p3) for which the estimated population of the bound form, p_{bound}, ranges from 0.2 to 0.7 for both proteins. Exchange between the two forms is fast on the chemical shift timescale (Figure S2 in the Supporting Information). Assuming this timescale is slower than the characteristic rotational diffusion of the complex, the measured R_1 is given by Equation (1).

$$R_1^{exp} = p_{bound} R_1^{bound} + (1 - p_{bound}) R_1^{free} \quad (1)$$

R_2 obeys a similar relationship, with additional R_{ex} contributions in the sites that experience chemical shift changes upon interaction [Eq. (2)].

$$R_2^{exp} = p_{bound} R_2^{bound} + (1 - p_{bound}) R_2^{free} + R_{ex} \quad (2)$$

[*] Dr. L. Salmon, A. Licinio, Dr. M. R. Jensen, Dr. M. Blackledge
Protein Dynamics and Flexibility, Institute de Biologie
Structurale Jean-Pierre Ebel, CNRS-CEA-UJF UMR 5075
41 rue Jules Horowitz, 38027-Grenoble Cedex (France)
Fax: (+33) 4-3878-9554
E-mail: malene.ringkjobing-jensen@ibs.fr
martin.blackledge@ibs.fr
Dr. J.-L. Ortega Roldan
Departamento de Química Física
e Instituto de Biotecnología, Facultad de Ciencias
Universidad de Granada
Granada (Spain)
Prof. N. van Nuland
Structural Biology Brussels, Vrije Universiteit Brussel
Pleinlaan 2, Brussels (Belgium)
and
Department of Molecular and Cellular Interactions, VIB
Pleinlaan 2, 1050 Brussels (Belgium)
Dr. E. Lescop
Centre de Recherche de Gif
Institut de Chimie des Substances Naturelles, CNRS
1 Avenue de la Terrasse, 91198 Gif sur Yvette (France)

[**] This work was supported by the ANR (PCV Protein Motion).

Supporting information for this article is available on the WWW under http://dx.doi.org/10.1002/anie.201100310.

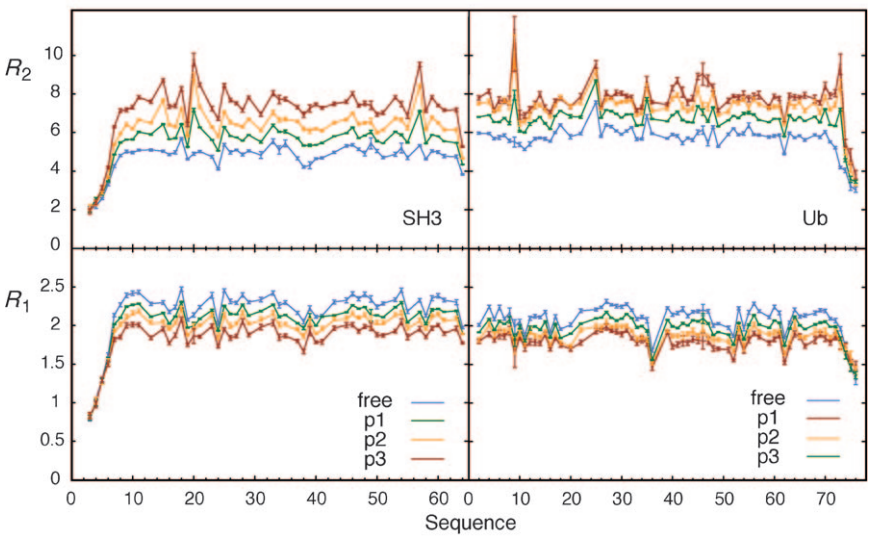

Figure 1. Experimental longitudinal and transverse ^{15}N relaxation rates (s^{-1}) in the two proteins measured at 308 K and 14.1 T for the free forms and three different mixtures.

R_{ex} is defined by the known expressions for contributions to transverse relaxation in the presence of a CPMG-based R_2 experiment (CPMG = Carr–Purcell–Meiboom–Gill; see the Supporting Information). R_1 values from the two partners were fitted to all points and extrapolated to the expected values in the bound form. Although a more complex regime has been proposed for a related SH3–Ub complex,[17] we have restricted our analysis to a two-state model. The actual bound fraction in the complex was simultaneously refined for both proteins along with the K_D. Chemical shifts from the different mixtures were incorporated into this fit, with limiting values in the free and bound forms fixed to those obtained from the K_D titration (Figure S4 in the Supporting Information). Examples of linear fits to the R_1 values are shown in Figure 2 A,E.

In theory a similar approach can be applied to R_2, with the possible presence of an additional R_{ex} contribution that gives rise to a deviation from the linearity with respect to the actual bound fraction in the complex. This will be manifest as a skewed bell-shaped distribution, the form of which depends on the off-rate of the interaction (k_{off}) and on the protein concentrations (Figure S1 in the Supporting Information). For dissociation constants similar or weaker to that studied here, it is impossible, in a viable concentration range, to experimentally isolate mixtures where the bound fraction is above 75%. The curvature of this dependence is in practice therefore difficult to determine from experimental data unless very specific exchange conditions are encountered.

We have therefore identified the exchange contributions in each mixture by using a hybrid Lipari–Szabo-type analysis of the relaxation data.[18] Effective rotational diffusion tensors were determined from the R_2/R_1 ratios from both partners for each fraction, which report on the population-weighted average of the diffusion tensors from free and bound forms of the proteins.[19,20] This gives rise to an artificial second rank tensor for each protein in each equilibrium mixture that governs the orientational relationship between the dominant relaxation-active mechanisms (the internuclear ^{15}N–^{1}H vectors) and the population-weighted R_2/R_1 ratios. This tensor can be determined and, as long as the diffusion tensors for the free and the bound states are in the same range, a pseudo-model-free analysis, which is based only on R_2 and R_1, can be performed by using this tensor to detect exchange contributions. In this case, the relaxation rates are fitted by using known expressions incorporating the spectral density function [Eq. (3)],

$$J(\omega) = \frac{2}{5}\sum_{r=1}^{5} A_r \frac{S^2\tau_r}{1+(\omega\tau_r)^2} + \frac{(1-S^2)\tau_i}{1+(\omega\tau_i)^2} \qquad (3)$$

where the A_r terms describe the orientational information encoded in the structure, τ_r gives the effective correlation times which define the anisotropic tensor,[21] and S^2 and τ_i represent the

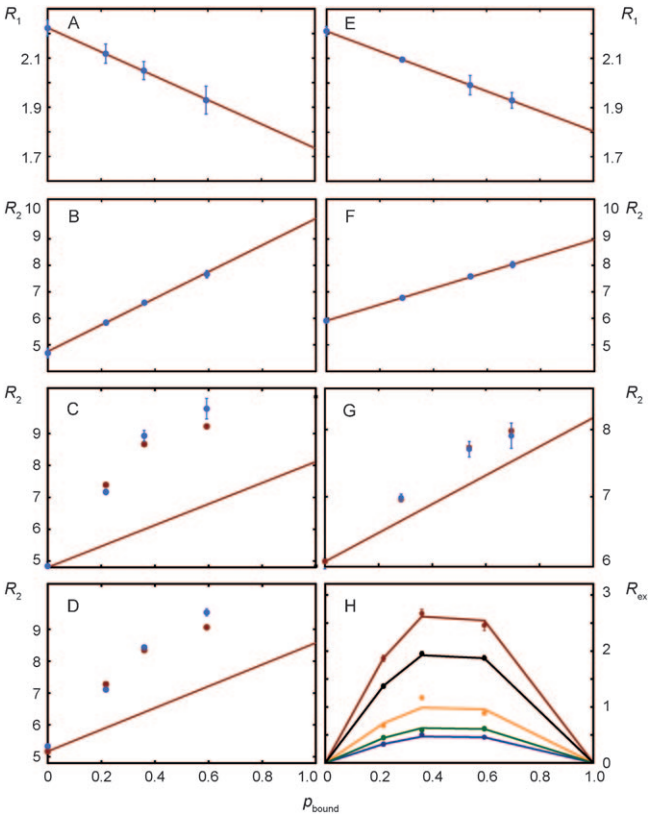

Figure 2. ^{15}N Relaxation rates (s^{-1}) measured for different equilibrium mixtures of Ub and SH3. A,E) Linear fit of the R_1 values comprising data from free proteins, and mixtures p1, p2, and p3 (A: SH3 Gly17, E: Ub Asn25). B,F) Linear fit of the R_2 values for sites with no R_{ex} (B: SH3 Gly42, F: Ub Val17). C,D,G) Linear fit of the R_2-R_{ex} values (red lines) for sites experiencing exchange (C,D: SH3 Asn20, Asp57, G: Ub Arg54). Blue dots: experimental values, red dots: fitted values. H) Fitted R_{ex} values with respect to p_{bound} for SH3 Thr18, Asp21, Tyr15, Asp57, and Asn20 (from bottom to top).

internal mobility. The R_{ex} value contributes only to R_2 and is invoked as an additional parameter where necessary. To illustrate the accuracy of the approach, high-resolution structures of the free forms of the proteins, in the relative orientation that was recently determined by using RDC-based refinement of the complex, were compared to the extrapolated values determined here.[22]

The experimental relaxation rates were analyzed to determine whether they could be reproduced within the experimental uncertainty, by using the Lipari–Szabo-type model-free approach [Eq. (3)]. Residue-specific models that incorporate S^2, τ_i, and R_{ex} were compared by strict statistical testing of models of increasing complexity using the program Tensor2.[23] This procedure identifies sites with significant exchange contributions for each mixture.[24,25] If a site was found to require R_{ex} for all mixtures, and not for the isolated forms of the proteins, these values were subtracted from the measured R_2 and linearly extrapolated to the fully bound form (Figure 2) As expected, these sites correlate well with those showing chemical shift perturbation upon interaction (Figure S3 in the Supporting Information). The dependence of the R_{ex} terms with respect to the population of both partners results in an estimated k_{off} value of $(1564 \pm 35)\ s^{-1}$ (Figure 2H shows the simultaneous fit of five sites).

The dependence of the experimental R_2/R_1 ratios with respect to the sequence for all fractions, and the extrapolated values in the complex, are shown in Figure 3 for SH3 (a similar dependence is seen for data from ubiquitin). The values are compared to those calculated from the optimal effective tensor and fitted using Equation (3). The different range of the R_2/R_1 ratios results from different rotational diffusion anisotropies of the free protein and the complex (eigenvalues shown in the legend). The good reproduction of experimental and extrapolated values indicates that fluctuations along the sequence derive mainly from the orientation of the bonds with respect to the axes of the effective tensor.

The diffusion tensors for both proteins in the complex are presented in Table 1. The eigenvalues are almost identical,

Table 1: Rotational diffusion tensors for the individual proteins in the complex (Ub, SH3) and for both partners together (Cp). Molecules were placed in a common referential axis system with their relative orientations as defined from a previous study in which RDCs and chemical shift titration were applied.

	$D_{\parallel}$ [$10^7\ s^{-1}$]	$D_{\perp}$ [$10^7\ s^{-1}$]	θ [°]	ϕ [°]	χ^2/N[a]
Ub	3.00 ± 0.02	2.31 ± 0.01	-46.1 ± 1.4	83.0 ± 1.4	76/54
SH3	2.96 ± 0.02	2.31 ± 0.01	-43.8 ± 1.3	85.4 ± 1.5	53/48
Cp	2.99 ± 0.03	2.31 ± 0.01	-44.6 ± 1.4	84.6 ± 1.3	137/102

[a] N is the number of points fitted. By using HydroNMR the tensor of the complex is: $(D_{\parallel}, D_{\perp}) = (2.9, 1.9)\ 10^7\ s^{-1}$, $(\theta, \phi) = (-44, 81)°$.

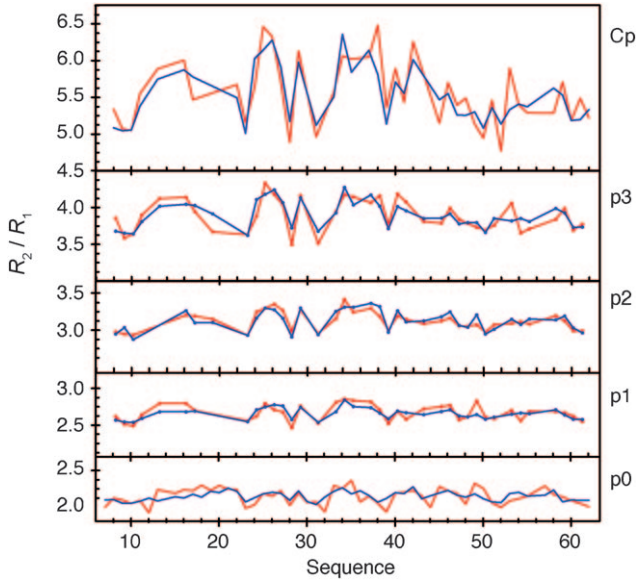

Figure 3. Experimental R_2/R_1 ratios (red lines) for all fractions of SH3. The p_{bound} values were determined to be: p0: 0.0, p1: 0.217, p2: 0.360, p3: 0.593. Extrapolated values in the complex (Cp). Sites exhibiting significant exchange are not shown. Blue lines: calculated values for optimal effective diffusion tensors (p0: $D_{\parallel} = 5.9 \times 10^7\ s^{-1}$, $D_{\perp} = 4.8 \times 10^7\ s^{-1}$, p1: $D_{\parallel} = 4.8 \times 10^7\ s^{-1}$, $D_{\perp} = 3.9 \times 10^7\ s^{-1}$, p2: $D_{\parallel} = 4.2 \times 10^7\ s^{-1}$, $D_{\perp} = 3.4 \times 10^7\ s^{-1}$, p3: $D_{\parallel} = 3.5 \times 10^7\ s^{-1}$, $D_{\perp} = 2.9 \times 10^7\ s^{-1}$).

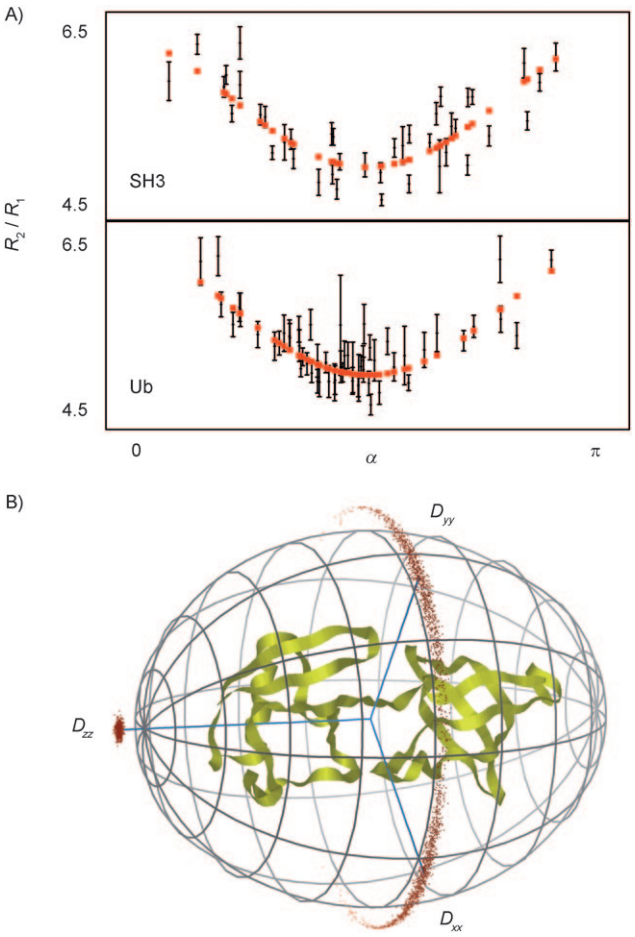

Figure 4. A) Angular dependence of the extrapolated R_2/R_1 ratios in the complex relative to the unique axis of the axially symmetric diffusion tensor. Error bars are centered at experimental points, red dots are calculated using the optimal tensor. The Pearson correlation coefficients are 0.92 and 0.87 for Ub and SH3, respectively. B) Representation of the diffusion tensor relative to the structure of the complex. Distributions of axis orientations, determined from Monte Carlo simulations, are shown as red dots.

and the tensors are found to be axially symmetric (no improvement is found when a fully anisotropic tensor is used). This complex was studied using a related titration approach, in which RDC values of different fractions of the partners were measured, and the values in the complex were determined similarly. The eigenvectors in the molecular frame, defined by the RDC-refined structure of the complex, are identical within experimental uncertainty, and similar to those calculated by HydroNMR.[26] The fit is of equal quality using both proteins together or separately. Figure 4A shows the dependence of the extrapolated R_2/R_1 ratios on the angle (α) of the internuclear vector with respect to the axis of the diffusion tensor.[27] The relative dimensions of the axes of the diffusion tensor are visualized (Figure 4B) with respect to the RDC-refined structure. Noise-based Monte Carlo simulations indicate the precision of the orientation of the diffusion tensor axes.

Figure 5 shows the comparison between the extrapolated R_2/R_1 ratios and the RDCs determined from the study of the complex when aligned in a sterically aligning liquid-crystal medium. Considering that neither data set were experimentally measured from the isolated complex, the similarity between the data sets resulting from partial alignment and anisotropic rotational diffusion in free solution, although expected,[28] is quite striking. This provides further evidence that the extrapolation techniques applied in these studies are accurate and precise. Refinement of the structure of the complex by using the program Sculptor[29] against these ratios, in combination with ambiguous chemical shift restraints used to raise the remaining orientational degeneracies (head to tail and about the tensor axis), determines the same relative orientation of the domains.

Finally, the availability of relaxation rates emanating from the bound form of a very weak complex allows for a direct comparison of the fast local dynamics which occur in the free and bound protein. We have determined the motional characteristics of both SH3 and Ub using the extrapolated rates, obtained by a model-free analysis. In this case the different τ_r values represent the effective correlation times which define the anisotropic diffusion tensor of the free and the bound forms of the protein. The results are shown in Figure 6 in terms of order parameters of the NH bond vectors,

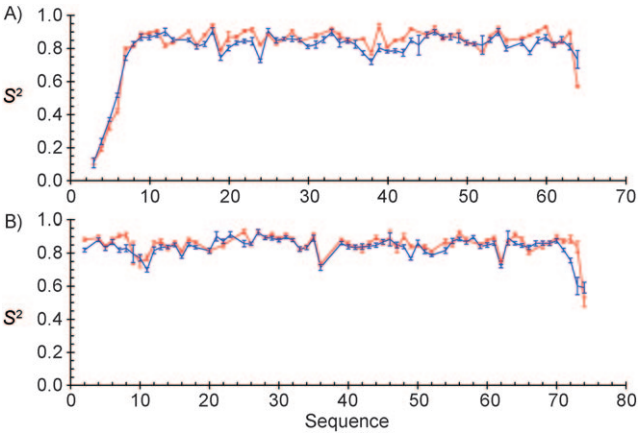

Figure 6. Internal mobility in the free and bound forms of SH3 (A) and Ub (B). Hybrid Lipari–Szabo-type analyses using spectral density functions of the form in Equation (3) were performed to determine the NH bond vector order parameters (blue: free forms, red: bound forms) by the program Tensor2.

indicating a very similar distribution of motions in the two forms of both proteins, but revealing an increase in rigidity in the C terminus of Ub, which interacts with SH3.

In conclusion, we have presented a general procedure for the characterization of weak protein–protein interactions that cannot easily be studied under saturating conditions. We demonstrate that the measurement of spin relaxation changes upon mixing of partner concentrations in the equilibrium mixture leads to accurate determination of the relaxation rates from the bound forms of both partners. These parameters are experimentally unattainable because of the difficulty of isolating the signal from the bound forms of the proteins. The method is applicable to a large number of protein complexes that are routinely studied by classical NMR chemical shift perturbation. Critically, however, this approach goes further, by simultaneously determining the long-range structure, internal dynamics, and kinetic parameters of weak protein complexes. This technique extends the unique capacity of NMR spectroscopy to determine the molecular basis of the largely unexplored binding modes of transient protein interactions.

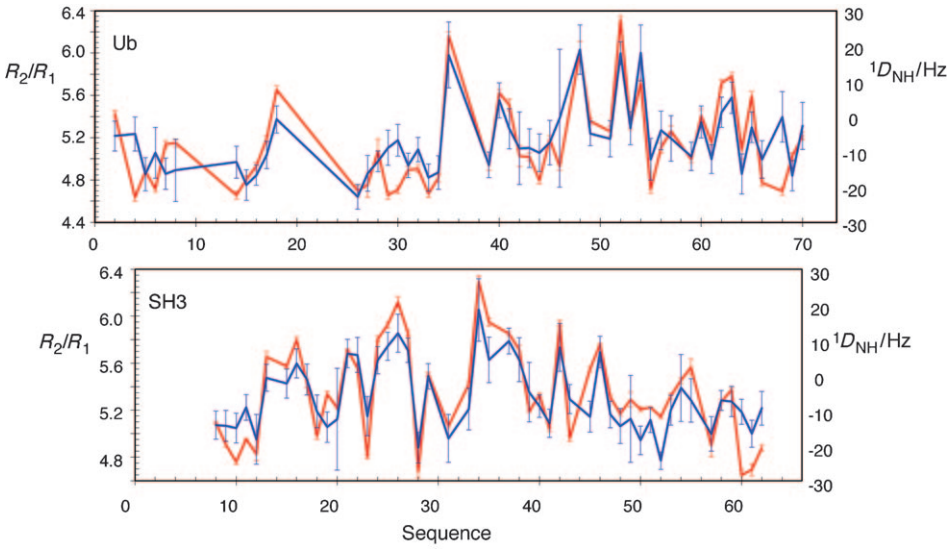

Figure 5. Comparison between extrapolated RDCs (red lines), derived from equilibrium mixtures of the complex, with extrapolated R_2/R_1 values using the current approach (blue lines) based on the measurement of ^{15}N spin relaxation rates (s^{-1}).

Received: January 13, 2011
Published online: March 18, 2011

Keywords: kinetics · molecular dynamics · NMR spectroscopy · protein–protein interactions · spin relaxation

[1] W. Kelly, M. Stumpf, *Curr. Opin. Biotechnol.* **2008**, *19*, 396 – 403.
[2] R. B. Russell, F. Alber, P. Aloy, F. P. Davis, D. Korkin, M. Pichaud, M. Topf, A. Sali, *Curr. Opin. Struct. Biol.* **2004**, *14*, 313 – 324.
[3] J. Vaynberg, J. Qin, *Trends Biotechnol.* **2006**, *24*, 22 – 27.
[4] J. Iwahara, G. M. Clore, *Nature* **2006**, *440*, 1227 – 1230.
[5] C. Dominguez, R. Boelens, A. M. J. J. Bonvin, *J. Am. Chem. Soc.* **2003**, *125*, 1731 – 1737.
[6] O. F. Lange, N. Lakomek, C. Farès, G. F. Schröder, K. F. A. Walter, S. Becker, J. Meiler, H. Grubmüller, C. Griesinger, B. L. de Groot, *Science* **2008**, *320*, 1471 – 1475.
[7] L. Salmon, G. Bouvignies, P. Markwick, N. Lakomek, S. Showalter, D. Li, K. Walter, C. Griesinger, R. Brüschweiler, M. Blackledge, *Angew. Chem.* **2009**, *121*, 4218 – 4221; *Angew. Chem. Int. Ed.* **2009**, *48*, 4154 – 4157.
[8] P. R. L. Markwick, G. Bouvignies, L. Salmon, J. A. McCammon, M. Nilges, M. Blackledge, *J. Am. Chem. Soc.* **2009**, *131*, 16968 – 16975.
[9] J. L. Ortega-Roldan, M. R. Jensen, B. Brutscher, A. I. Azuaga, M. Blackledge, N. A. J. van Nuland, *Nucleic Acids Res.* **2009**, *37*, e70.
[10] R. Brüschweiler, X. Liao, P. E. Wright, *Science* **1995**, *268*, 886 – 889.
[11] N. Tjandra, D. S. Garrett, A. M. Gronenborn, A. Bax, G. M. Clore, *Nat. Struct. Biol.* **1997**, *4*, 443 – 449.
[12] P. Tsan, J. Hus, M. Caffrey, D. Marion, M. Blackledge, *J. Am. Chem. Soc.* **2000**, *122*, 5603 – 5612.
[13] D. Fushman, R. Varadan, M. Assfalg, O. Walker, *Prog. Nucl. Magn. Reson. Spectrosc.* **2004**, *44*, 189 – 214.
[14] A. D. J. van Dijk, D. Fushman, A. M. J. J. Bonvin, *Proteins Struct. Funct. Genet.* **2005**, *60*, 367 – 381.
[15] N. Tjandra, S. Feller, R. Pastor, A. Bax, *J. Am. Chem. Soc.* **1995**, *117*, 12562 – 12566.
[16] J. Ortega Roldan, M. Romero, A. Ora, E. Ab, O. Mayorga, A. Azuaga, N. van Nuland, *J. Biomol. NMR* **2007**, *39*, 331 – 336.
[17] D. M. Korzhnev, I. Bezsonova, S. Lee, T. V. Chalikian, L. E. Kay, *J. Mol. Biol.* **2009**, *386*, 391 – 405.
[18] G. Lipari, A. Szabo, *J. Am. Chem. Soc.* **1982**, *104*, 4559 – 4570.
[19] D. Fushman, S. Cahill, D. Cowburn, *J. Mol. Biol.* **1997**, *266*, 173 – 194.
[20] P. Bernadó, T. Akerud, J. de La Torre, M. Akke, M. Pons, *J. Am. Chem. Soc.* **2003**, *125*, 916 – 923.
[21] D. Woessner, *J. Chem. Phys.* **1962**, *37*, 647 – 654.
[22] G. Cornilescu, J. Marquardt, M. Ottiger, A. Bax, *J. Am. Chem. Soc.* **1998**, *120*, 6836 – 6837.
[23] P. Dosset, J. C. Hus, M. Blackledge, D. Marion, *J. Biomol. NMR* **2000**, *16*, 23 – 28.
[24] A. Mandel, M. Akke, A. Palmer, *J. Mol. Biol.* **1995**, *246*, 144 – 163.
[25] S. M. Kristensen, G. Siegal, A. Sankar, P. C. Driscoll, *J. Mol. Biol.* **2000**, *299*, 771 – 788.
[26] P. Bernadó, J. de La Torre, M. Pons, *J. Biomol. NMR* **2002**, *23*, 139 – 150.
[27] M. Blackledge, F. Cordier, P. Dosset, D. Marion, *J. Am. Chem. Soc.* **1998**, *120*, 4538 – 4539.
[28] E. de Alba, J. Baber, N. Tjandra, *J. Am. Chem. Soc.* **1999**, *121*, 4282 – 4283.
[29] H. Wu, M. Blackledge, M. W. Maciejewski, G. P. Mullen, S. M. King, *Biochemistry* **2003**, *42*, 57 – 71.

